Earth Syst. Dynam. Discuss., 2, 133–159, 2011
www.earth-syst-dynam-discuss.net/2/133/2011/
doi:10.5194/esdd-2-133-2011

Earth System Dynamics Discussions

Role of volcanic forcing on future global carbon cycle

J. F. Tjiputra[1,2] **and O. H. Otterå**[2]

[1]Geophysical Institute, University of Bergen, Bergen, Norway
[2]Uni Research, Bjerknes Center for Climate Research, Bergen, Norway

Received: 8 February 2011 – Accepted: 14 February 2011 – Published: 16 February 2011

Correspondence to: J. F. Tjiputra (jtj061@uib.no)

Published by Copernicus Publications on behalf of the European Geosciences Union.

Abstract

Using a fully coupled global climate-carbon cycle model, we assess the potential role of volcanic eruptions on future projection of climate change and its associated carbon cycle feedback. The volcanic-like forcings are applied together with business-as-usual IPCC-A2 carbon emissions scenario. We show that very large volcanic eruptions similar to Tambora lead to short-term substantial global cooling. However, over a long period, smaller but more frequent eruptions, such as Pinatubo, would have a stronger impact on future climate change. In a scenario where the volcanic external forcings are prescribed with a five-year frequency, the induced cooling immediately lower the global temperature by more than one degree before return to the warming trend. Therefore, the climate change is approximately delayed by several decades and by the end of the 21st century, the warming is still below two degrees when compared to the present day period. The cooler climate reduces the terrestrial heterotrophic respiration in the northern high latitude and increases net primary production in the tropics, which contributes to more than 45% increase in accumulated carbon uptake over land. The increased solubility of CO_2 gas in seawater associated with cooler SST is offset by reduced CO_2 partial pressure gradient between ocean and atmosphere, which results in small changes in net ocean carbon uptake. Similarly, there is nearly no change in the seawater buffer capacity simulated between the different volcanic scenarios. Our study shows that even in the relatively extreme scenario where large volcanic eruptions occur every five-years period, the induced cooling only leads to a reduction of 46 ppmv atmospheric CO_2 concentration as compared to the reference projection of 878 ppmv, at the end of the 21st century. With respect to sulphur injection geoengineering method, our study suggest that small scale but frequent mitigation is more efficient than the opposite. Moreover, the longer we delay, the more difficult it would be to counteract climate change.

ESDD
2, 133–159, 2011

1 Introduction

Future climate change is expected to vary considerably according to the rate of anthropogenic carbon emissions and uptake by both the ocean and the terrestrial biosphere. Earth system models contain sophisticated interactions between the atmospheric and oceanic physics coupled with the global carbon cycle. They can be used to simulate and predict how future climate would evolve under a given anthropogenic greenhouse gas emission scenario. Recent studies using such models have indicated that future climate change will reduce the efficiency of the Earth system to absorb the emitted anthropogenic carbon, and would hence provide a positive feedback (Friedlingstein et al., 2006; Crueger et al., 2008; Tjiputra et al., 2010). Those studies, however, did not take into account not yet predictable factors such as volcanic eruptions or similar external forcings.

Volcanic forcing is well known to induce negative radiative forcing following the eruptions (Hansen et al., 1996; Gregory, 2010). Recent studies have also emphasized the crucial role of volcanic eruptions in controlling the global climate variability in the past (Otterå et al., 2010; Stenchikov et al., 2009). Explosive volcanic eruptions inject a large amount of different types of particles and gases into the stratosphere, such as ash, water vapour (H_2O), carbon dioxide (CO_2), and sulfur dioxide (SO_2). Most of the ash will be washed out of the troposphere quite rapidly, on time scales of minutes to a few weeks. Gases such as H_2O and CO_2 are important greenhouse gases, but their atmospheric concentrations are so large that individual eruptions have a minimal effect upon the overall concentrations and thus do not directly impact the greenhouse effect.

The most important climatic effect of explosive volcanic eruptions is through the emission of sulphur species, mostly as SO_2, into the stratosphere. The SO_2 is rapidly converted into sulphuric acid, which in turn condenses into aerosols. These volcanic aerosols are then spread around the globe by atmospheric circulation and produce aerosol clouds that scatter more incoming solar radiation back to the space, resulting in cooler surface temperatures. In addition, volcanic aerosols also absorb both solar

ESDD
2, 133–159, 2011

and terrestrial radiation, which heat the stratosphere (Robock, 2000). The resulting perturbation to the Earth's radiative balance, in turn, alters the atmospheric circulation and other climate parameters. However, the large reduction in direct shortwave radiation reaching the surface is the primary response of the volcanic aerosols resulting in a net surface and hence global cooling.

Sulfate aerosols resulting from strong volcanic explosions last for 3-5 years in the lower stratosphere. Therefore, it has traditionally been believed that volcanic impacts produce mainly short-term, transient climate perturbations. However, the ocean integrates volcanic radiative cooling and responds over a wide range of time scales. Some recent model studies indicate that very large eruptions or a clustering of major eruptions may represent a substantial climate forcing over decadal to multi-decadal time scales (Stenchikov et al., 2009; Otterå et al., 2010). In these studies key variables in the Atlantic climate system such as sea ice and the ocean circulation are found to be quite sensitive to volcanic forcing. The associated processes, especially ocean heat uptake, play a key role in ongoing climate change. An improved assessment of possible long-term climate effects of volcanic eruptions is therefore important in order to put the ongoing climate change into a proper context.

By perturbing the climate system, volcanic eruption will alter the global carbon cycle as well. Studies by Sarmiento (1993) and Jones and Cox (2001) show a measurable change in the atmospheric CO_2 concentration growth rate following the 1991 Mount Pinatubo eruption, which cannot be explained by the changes in anthropogenic carbon emissions alone. A further study by Bousquet et al. (2000) indicates an additional carbon sink of about 2 Pg C in response to the Pinatubo eruption.

Due to the counteracting effect of volcanic eruptions on anthropogenic climate change and atmospheric CO_2 concentration, several geoengineering options for climate change mitigation mimicking the volcanic eruptions have been recently proposed and studied (e.g., Crutzen, 2006; Wigley, 2006; Rasch et al., 2008; Robock et al., 2008, 2010; Moore et al., 2010). However, the impact and feedback of such large-scale geoengineering schemes on the Earth system remain poorly understood. Observational

ESDD
2, 133–159, 2011

data indicate that the Pinatubo eruption had a large impact on regional climate resulting for instance in large-scale changes in the monsoons (Trenberth and Dai , 2007). This could potentially lead to droughts in large parts of the globe, which would affect millions of people. More detailed assessment is undoubtedly needed before one could consider the method as promising or would have to reject it. Climate models offer the ideal laboratory to perform such sulfur injection schemes in a controlled environment, and systematically assess potential impacts on climate and environment. In this study, we focus on the role of future volcanic-like forcing on the global carbon cycle. For this purpose, we adopt the Bergen Earth system model (BCM-C), which consists of a fully interactive climate model coupled with oceanic and terrestrial carbon cycle models.

Whilst a model study by Brovkin et al. (2010) has analyzed the sensitivity of the global carbon cycle to large volcanic eruptions in the historical period, our study offers a new perspective on how future episodic volcanic eruptions would influence the carbon cycle and the associated feedback to the increasing atmospheric CO_2 concentration projected under the SRES-A2 emission scenario.

The paper is organized as follows. The next section will describe the model and experiment design adopted in this study. The third section will discuss our experiment results for each the terrestrial and oceanic carbon cycles. The final section includes a discussion and a summary of the paper.

2 Method

2.1 Model description

The Bergen Earth system model (BCM-C) is used in this study. It is an updated version of the Bergen Climate Model (BCM; Furevik et al., 2003) coupled with terrestrial and oceanic carbon cycle models. The atmospheric component is ARPEGE-Climat version 3 with a truncation at wave number 63 (TL63) and 1800 s time step. A total of 31 vertical levels, ranging from the surface to 0.01 hPa are employed. The current

ESDD
2, 133–159, 2011

version differs from the original BCM in that the vertical diffusion scheme has been updated to that of ARPEGE-Climat version 4 (Otterå et al., 2009). The ocean component is a modified version of MICOM (Bleck and Smith, 1990; Bleck et al., 1992; Bentsen et al., 2004), an isopycnic ocean GCM. It has approximately 2.4° × 2.4° horizontal resolution with 34 isopycnic vertical layers. The model adopts a single non-isopycnic surface mixed layer, which provides the linkage between the atmospheric forcing and the ocean interior. The ocean carbon cycle model is the Hamburg oceanic carbon cycle (HAMOCC5) model (Maier-Reimer et al., 2005). The HAMOCC5 model simulates carbon chemistry and includes an NPZD-type (nutrient, phytoplankton, zooplankton, and detritus) ecosystem model. Finally, the terrestrial model is the Lund-Potsdam-Jena (LPJ) model (Sitch et al., 2003). The LPJ is a large-scale dynamic vegetation model comprises of 10 plant functional types. A more detailed description of the BCM-C model and its evaluation are available in Tjiputra et al. (2010).

In all simulations, the BCM-C is interactively coupled with the carbon cycle modules with no flux adjustments applied. In order to simulate volcanic eruptions, sulphur aerosols are injected directly into the stratosphere. The volcanic aerosol time series is supplied as monthly optical depths at 0.55 microns, in the middle of the visible spectrum (Crowley et al., 2003). The forcing were applied as quarterspheric (30° N–90° N, 0–30° N, 30° S–0, 90° S–30° S) monthly values, and distributed in each model level in the stratosphere (Otterå, 2008). The volcanic mass of the stratospheric aerosols are calculated at each grid point and model level in the stratosphere by dividing the total aerosol concentration by the total air mass of all stratospheric levels at that grid point.

The atmosphere model ARPEGE (i.e., the atmospheric component of the BCM-C) is able to reproduce many of the observed features after the Mount Pinatubo eruption (Otterå, 2008). Both the simulated shortwave and longwave reductions as well as the general global cooling after the eruption compares favorably with observations. In addition, the observed winter warming pattern over NH land is well captured. This winter warming was caused by an anomalously positive phase of the Arctic Oscillation (AO) associated with the enhanced Equator-to-pole temperature gradient in the stratosphere

ESDD
2, 133–159, 2011

that developed due to aerosol heating of the tropics. Similarly, the opposite summer cooling observed is also produced by the model. Finally, a strong response of the AO/NAO to historical volcanic forcing in BCM (i.e. in coupled mode) has been further confirmed in a long transient simulation of the last 600 years (Otterå et al., 2010).

2.2 Experiment design

A total of three model simulations are performed with the BCM-C model. Prior to the model simulations, the model has been spun up for more than 600-years based on constant preindustrial atmospheric CO_2 concentration of 284.7 ppmv. Afterwards, the fully coupled model is simulated from year 1850 to 2019 forced only by prescribed historical and the SRES-A2 CO_2 emission time series (Marland et al., 2005; Houghton and Hackler, 2002). The model is then branched out into three separate simulations, while still prescribing the A2 emissions scenario toward the end of the 21st century.

In the first branch, no external forcing is applied, hence it serves as a reference simulation, REF. Next we pick two historical volcanic eruptions from the volcanic forcing data set of Crowley et al. (2003) and construct two alternative scenarios. In the second branch, a volcanic eruption corresponding to the Tambora 1815 historical eruption is applied in 25-year intervals, starting from year 2025, GEO_TAM. Finally, in the third branch, a relatively weaker volcanic eruption corresponding to the Pinatubo 1991 eruption is applied in 5-year intervals, starting from year 2020, GEO_PIN. Figure 1 illustrates the aerosol loading applied in experiments GEO_TAM and GEO_PIN. Table 1 summarizes the descriptions of all three model simulations.

Note that natural volcanic eruptions also release greenhouse gases such as H_2O and CO_2, but both in negligible amounts compared to the associated concentrations in the current atmosphere. Thus, only sulfur aerosols are included in this study. The BCM-C future projection and climate–carbon cycle feedback under the SRES-A2 have been evaluated and is well within the range of other models (Friedlingstein et al., 2006; Tjiputra et al., 2010).

ESDD
2, 133–159, 2011

3 Results

The volcanic forcing in the model simulations induces cooler surface temperatures immediately following the perturbation. The largest cooling is simulated over high latitudes, particularly the Northern Hemisphere, which results in an enhanced pole-to-equator temperature gradient similar to Robock (2000).

In GEO_TAM, the volcanic forcings induce an average of approximately one degree cooling in the simulated global mean surface temperature immediately follow the eruption events. Similar cooling patterns, which are followed by rapid warming, are also generated in the sea surface temperature. Figure 2 shows that the cooling effect in GEO_TAM only lasts for a few years before the air and SST temperatures return to the expected warming trends as seen in REF.

In GEO_PIN, the simulated cooling effect is weaker than in GEO_TAM. However, due to continuous cooling during the first few volcanic events, the overall persisted warming trend is delayed by several decades. Figure 2 also shows that the warming rate in GEO_PIN is not as sharp as in the REF with the simulated global air temperature being approximately one degree lower.

Similar to the temperature, the global mean precipitation also experiences perturbations. The cooler climate leads to reduced global precipitation with similarly stronger signals in the GEO_TAM run. Interestingly, by the end of the 21st century, GEO_PIN simulates relatively small changes in global precipitation relative to period before the volcanic forcings are introduced (i.e., year 2019), despite the fact that considerable change in SST and air temperature are predicted. Figure 2 also illustrates that in both GEO_TAM and GEO_PIN the Arctic sea ice extent and the Atlantic Meridional Overturning Circulation (AMOC) are expected to decrease toward the end of the experiment period, closely following the REF simulation.

With regards to the global carbon cycle, there are noticeably increases in both the oceanic and terrestrial carbon uptake following the volcanic forcings in GEO_TAM as compared to the REF. Nevertheless, both REF and GEO_TAM project virtually similar

ESDD
2, 133–159, 2011

atmospheric CO_2 concentration by the end of the 21st century (Fig. 3). Figure 3 also shows that the volcanic-like forcings induce temporary increases in oceanic and terrestrial carbon uptake, with the land uptake being more pronounced. The next subsection details the carbon cycle processes contribute to this change.

In the GEO_PIN, the volcanic forcings induce more pronounced change in terrestrial carbon uptake than the oceanic counterpart. For the 2020 to 2099 period, the model simulates accumulated oceanic and land carbon uptake of 373.1 and 313.9 Pg C, as compared to 377.0 and 215.9 Pg C simulated in REF. Therefore, to a first order, an increase in terrestrial carbon uptake in GEO_PIN could explained the simulated 45.6 ppmv lower atmospheric CO_2 concentration at the end of the 21st century (i.e., difference in terrestrial carbon uptake of 98 Pg C approximately corresponds to 46.9 ppmv).

Due to the relatively small changes simulated in GEO_TAM compare to REF, our post-eruption analysis will be focused more on the GEO_PIN results. The next subsections look into more detail of the mean climatic change and the carbon cycle variability following the eruption events.

3.1 Terrestrial carbon cycle

Fluxes of carbon between the atmosphere and the land are primarily controled by the difference between terrestrial photosynthesis (uptake) and heterothropic respiration (outgassing). In order to qualitatively analyze the regional change in climate and carbon cycle over land associated with the eruptions, we compute the latitudinal mean change in land surface air temperature, precipitation, net primary production (NPP), and soil respiration in the first, second, third, and fourth years after the volcanic events (Fig. 4). The mean deviation shown in Fig. 4 is computed from all 16 eruption events in GEO_PIN as compared to the year prior to each eruptions. The largest mean cooling period occurs immediately following the volcanic eruption (i.e., first year) with a reduction of nearly 1K simulated in some regions in the Northern Hemisphere. Afterwards the temperature steadily recovers to the pre-eruption level. Analogous to the cooling,

ESDD
2, 133–159, 2011

the model also simulates reductions in precipitation in the first year of a volcanic event, particularly in low latitudes. However, the changes in the precipitation pattern appear to be more complicated. This is consistent with study by Brovkin et al. (2010), which also demonstrates pronounced cooling over high latitude Northern Hemisphere landmasses. Also similar to their study, the model only simulates a small cooling in the Southern Hemisphere, essentially caused by the distinct land-to-ocean ratio between the two hemispheres.

Over the period when the volcanic forcings are applied, GEO_PIN simulates NPP and soil respiration reduction of approximately 27.7 and 122.8 Pg C as compared to the REF run. GEO_PIN also simulates slightly less accumulated carbon outgassing associated with fire fluxes of 2.4 Pg C. This strongly reduced respiration more than offsets the reduced NPP and essentially leads to increased net terrestrial carbon uptake of about 97.5 Pg C. By the end of the model simulation, the LPJ simulates increases in soil, litter and vegetation carbon masses by approximately 34.6, 13.8, and 48.8 Pg C, respectively in GEO_PIN when compared to REF.

The net carbon gain by the terrestrial biosphere occurs mostly in the tropics and mid-latitude Northern Hemisphere. We attribute the former to the increase in net primary production as shown in Fig. 4. On the other hand, the net carbon gain in the mid-latitude Northern Hemisphere is dominated by reduced soil respiration due to the simulated cooler temperature following the eruption events. An earlier modeling study by Jones and Cox (2001) feature similar mechanisms in the tropics associated with the Mount Pinatubo eruption. Figure 5 shows that the net primary production increase in the tropics leads to increase in carbon stored in the vegetation pool, whereas reduced respiration in the mid-latitude Northern Hemisphere leads to an increased soil carbon pool in these regions. Note that the injected aerosols also lead to a broad reduced incoming short-wave solar radiation (not shown) simulated in the model, but appear to have insignificant effect.

ESDD
2, 133–159, 2011

3.2 Oceanic carbon cycle

The global carbon uptake by the ocean is not perturbed substantially by the volcanic eruption forcings. Over the 2020–2099 period, experiments REF, GEO_TAM, and GEO_PIN simulate accumulated oceanic carbon uptake of 377.0, 377.1, and 373.1 Pg C, respectively. Nevertheless, regional changes would be expected as a result of changing climate. In the model, the carbon fluxes from the atmosphere to the ocean are formulated as a function of solubility, gas transfer rate, and difference in atmospheric and oceanic partial pressure CO_2 (pCO_2) following Wanninkhof (1992). Thus changes in atmospheric circulation and temperature would alter the solubility and gas transfer rate parameters in the model, whereas changes in terrestrial carbon fluxes would in addition contribute to an altered air-sea pCO_2 gradient. Changes in the gas transfer rate turns out to be relatively smaller than changes in solubility (not shown). Figure 6 shows that the solubility of CO_2 gas in seawater is expected to steadily decrease toward the end of the 21st century for all ocean regions, based on experiment REF. Cooling effects associated with volcanic eruption in GEO_TAM can be clearly detected, increasing the solubility only temporarily for a few years following the eruptions and returning to the decreasing trend as in REF. In GEO_PIN, more frequent volcanic forcings are able to increase and maintain high solubility until the mid-21st century before they start to decrease. Interestingly, in the high latitude Southern Ocean, the solubility parameter appears to recover towards the end of experiment period.

Despite the delayed solubility reduction simulated in GEO_PIN, there is no significant increase in global oceanic carbon uptake (see also Fig. 3). In fact, GEO_PIN simulates 4 Pg C less than the REF. We attribute this to the reduction in the atmospheric CO_2 concentration, associated with a stronger carbon uptake by the terrestrial compartment. This lower atmospheric CO_2 concentration reduced the pCO_2 gradient between the ocean and atmosphere, thus weakening the oceanic uptake strength.

ESDD
2, 133–159, 2011

Another way to explain the relatively small change in the oceanic carbon uptake to the volcanic forcings is through the Revelle factor. The Revelle factor is computed as the change of pCO_2 in seawater for a given change in surface concentration of dissolved inorganic carbon (DIC). Its value is indirectly proportional to atmospheric CO_2 concentration and reversely proportional to the temperature of the seawater (Zeebe and Wolf-Gladrow, 2001). Therefore, given the same atmospheric CO_2 concentration, low latitude oceans generally have lower Revelle factors whereas high latitude oceans have higher Revelle factors (Sabine et al., 2004). Seawater with high (low) Revelle factor has low (high) buffer capacity of CO_2 in the associated water mass. For this reason, seawater with low Revelle factor has more capacity in taking up anthropogenic CO_2 from the atmosphere. Future climate change is associated with raising temperature and atmospheric CO_2 concentration. While higher sea surface temperature increase the buffer capacity, higher atmospheric CO_2 does the opposite. It is a balance between these two factors that control the future oceanic buffer capacity, hence the oceanic carbon uptake. Figure 7 shows the area-weighted regional evolution in the Revelle factor, estimated following Maier-Reimer and Hasselmann (1987). While Fig. 6 shows that the volcanic forcings alter the regional solubility of CO_2 in seawater considerably, there is principally no change in the simulated Revelle factor (except for the Arctic), which also explain that over large scale, the ocean takes up approximately similar amount of carbon between the three experiments in this study.

With respect to the marine ecosystem, a global decrease in biological production is expected in the future. Under warmer climate, stronger stratification and shallower mixed layer depth would lead to reduced surface nutrient, essential for marine productivity (Bopp et al., 2001; Steinacher et al., 2010). Reduced marine production lead to reduced export production, which is an important mechanism to transport carbon from surface to the deep water, also known as the "biological pump". By the end of the 21st century (i.e., averaged over 2090–2099), the REF run simulates a global export production of $8.0 \pm 0.2\,\mathrm{Pg\,C\,yr^{-1}}$, considerably lower compare to the pre-industrial value of $9.1 \pm 0.2\,\mathrm{Pg\,C\,yr^{-1}}$. Experiment GEO_TAM produces similar quantity

ESDD
2, 133–159, 2011

of $8.1 \pm 0.1\,\mathrm{Pg\,C\,yr^{-1}}$, whereas GEO_PIN maintains a relatively higher export production of $8.7 \pm 0.3\,\mathrm{Pg\,C\,yr^{-1}}$ at the end of this century, still within the preindustrial variability.

Since the ocean takes up approximately similar amounts of carbon for all experiments, the surface ocean is still projected by the model to acidify considerably to below 7.8 pH units, down by more than 0.35 pH units as compared to the preindustrial value.

4 Summary and discussion

Future climate and carbon uptake are projected using the Bergen Earth system model under the SRES-A2 emission scenario. To study the potential feedback associated with episodic volcanic forcings within the 21st century, multiple simulations were performed, applying two different scenarios of volcanic eruptions. In the first scenario, large volcanic eruptions, comparable to the 1815's Tambora, are prescribed for the year 2025, 2050, and 2075. On the other, slightly weaker eruptions, comparable to the 1991's Pinatubo, are prescribed occurring every five-years, starting from 2020.

Our experiments show that the feedback of the volcanic eruptions on the global carbon cycle is dominated by the terrestrial biosphere. Cooling over land leads to prolonged soil carbon turnover rate in mid-latitude Northern Hemisphere and increased vegetation carbon budget in low latitude, resulting in overall net carbon uptake. In some regions such as the polar Northern Hemisphere, the reduced soil respiration still prevails over the lowered photosynthesis rate. The enhanced carbon uptake by the land biosphere following a volcanic eruption is well supported by both modeling and inversion studies (Bousquet et al., 2000; Jones and Cox, 2001; Lucht et al., 2002; Brovkin et al., 2010) for the historical periods. Nevertheless, the regional uptake anomalies vary considerably between studies. For example, increased carbon content in the tropics is suggested by Jones and Cox (2001) and Brovkin et al. (2010), whereas study by Bousquet et al. (2000) indicates more terrestrial carbon uptake in the Northern Hemisphere regions (e.g., north of 45° N) due to eruptions induced cooling. Another study

ESDD
2, 133–159, 2011

by Lucht et al. (2002) using a similar dynamical vegetation model as the BCM-C also simulates high-latitude carbon uptake following the Pinatubo eruptions. Interestingly, the BCM-C simulates increased carbon content both in the tropics and Northern Hemisphere following the eruption events, probably due to the additional "CO_2 fertilisation effect" induced in our model's future projections.

Over the ocean, the volcanic eruptions reduce the ocean heat content, and consequently lower the projected SST (Gregory, 2010). This condition favour stronger atmospheric CO_2 uptake because the solubility of CO_2 gas is higher in colder water, though the solubility effect is partly counteracted by a decrease in buffering ability at lower temperatures (less well occurring dissociation of carbonic acid into bicarbonate and carbonate). In addition, simultaneous and stronger terrestrial carbon uptake lead to a reduction in atmospheric CO_2, lowering the pCO_2 gradient between the atmosphere and the ocean. In a large-scale, all of these factors contribute to relatively small changes in the buffer capacity of the seawater, which resulted in small change in long-term oceanic carbon uptake.

Our study indicates that it would be in principle, and if no other reasons would speak against the procedure, more efficient to counteract global warming with small-scale and frequent sulphur injection rather than large-scale but less frequent operations. The experiments also show that geoengineering methods mimicking volcanic eruptions could offer some benefits to the Earth system, such as by delaying the future warming rate, increasing anthropogenic carbon uptake, and potentially sustaining marine productivity. While there may be some benefits associated with such a mitigation action, there are also many unanticipated and unknown consequences that could lead to potentially catastrophic consequences. For example, the potential stratospheric ozone destruction, potential acid rain, effects on cirrus clouds, impacts of the released volcanic dust on terrestrial and marine ecosystem (Sarmiento, 1993; Duggen et al., 2010), changes in ocean circulation that may need decades or centuries to recover, etc. All of these factors remain poorly understood, adding to the fact that the current technology is still in its infancy. Furthermore, the study by Matthews and Caldeira (2007) includes the

ESDD
2, 133–159, 2011

warning that, should geoengineering fail or stopped abruptly, it could lead to very rapid climate change, with warming rates up to 20 times greater than present-day rates. Even if such method can be deployed successfully, our study shows that high concentration of atmospheric CO_2 would remain in the atmosphere for a long time. And as our simulations do not produce considerable change in oceanic carbon uptake, the ocean is still expected to acidify considerably by the end of the 21st century. The current version of the LPJ also does not implement nitrogen limitation, which could alter the carbon uptake due to climate change (Bonan and Levis, 2010). Given the large uncertainties, the safest and best solution to counteract the current global warming problem is to reduce the anthropogenic carbon emissions substantially, and as soon as possible.

Acknowledgements. We thank Christoph Heinze for the discussions and valuable feedbacks on this manuscript, Caroline Roelandt for reviewing the early version of the manuscript. This study at the University of Bergen and Bjerknes Centre for Climate Research is supported by the Research Council of Norway funded project NorClim and CarboSeason (grant no. 185105/530), and the large-scale integrating EU FP7 project COMBINE (grant no. 226520). We acknowledge the Norwegian Metacenter for Computational Science and Storage Infrastructure (NOTUR and NorStore, "Biogeochemical Earth system modeling" project nn2980k and ns2980k) for providing the computing and storing resources essential for this study.

References

Bentsen, M., Drange, H., Furevik, T., and Zhou, T.: Simulated variability of the Atlantic meridional overturning circulation, Clim. Dynam., 22, 701–720, 2004. 138

Bleck, R. and Smith, L. T.: A wind-driven isopycnic coordinate model of the North and Equatorial Atlantic Ocean, 1. Model development and supporting experiments, J. Geophys. Res., 95, 3273–3285, 1990. 138

Bleck, R., Rooth, C., Hu, D., and Smith, L. T.: Salinity-driven Thermocline Transients in a Wind- and Thermohaline-forced Isopycnic Coordinate Model of the North Atlantic, J. Phys. Oceanogr., 22, 1486–1505, 1992. 138

Bonan, G. B. and Levis, S.: Quantifying carbon-nitrogen feedbacks in the community land model (CLM4), Geophys. Res. Lett., 37, L07401, doi:10.1029/2010GL042430, 2010. 147

ESDD

2, 133–159, 2011

Bopp, L., Monfray, P., Aumont, O., Dufresne, J.-L., Le Treut, H., Madec, G., Terray, L., and Orr, J. C.: Potential impact of climate change on marine export production, Global Biogeochem. Cy., 15, 81–99, 2001. 144

Bousquet, P., Peylin, P., Ciais, P., Le Quéré, C., Friedlingstein, P., and Tans, P. P.: Regional changes in carbon dioxide fluxes of land and oceans since 1980, Science, 290, 1342–1346, 2000. 136, 145

Brovkin, V., Lorenz, S. J., Jungclaus, J., Raddatz, T., Timmreck, C., Reick, C. H., Segschneider, J., and Six, K.: Sensitivity of a coupled climate-carbon cycle model to large volcanic eruptions during the last millennium, Tellus B, 62, 674–681, 2010. 137, 142, 145

Crowley, T., Baum, S. K., Kim, K.-Y., Hegerl, G. C., and Hyde, W. T.: Modeling ocean heat content changes during the last millennium, Geophys. Res. Lett., 30, 1932, 2003. 138, 139

Crueger, T., Roeckner, E., Raddatz, T., Schnur, R., and Wetzel, P.: Ocean dynamics determine the response of oceanic CO_2 uptake to climate change, Clim. Dynam., 31, 151–168, doi:10.1007/s00382-007-0342-x, 2008. 135

Crutzen, P. J.: Albedo enhancement by stratospheric sulfur injections: a contribution to resolve a policy dilemma?, Climatic Change, 77, 211–219, 2006. 136

Duggen, S., Olgun, N., Croot, P., Hoffmann, L., Dietze, H., Delmelle, P., and Teschner, C.: The role of airborne volcanic ash for the surface ocean biogeochemical iron-cycle: a review, Biogeosciences, 7, 827–844, doi:10.5194/bg-7-827-2010, 2010. 146

Friedlingstein, P., Cox, P., Betts, R., Bopp, L., von Bloh, W., Brovkin, V., Cadule, P., Doney, S., Eby, M., Fung, I., Gala, B., John, J., Jones, C., Joos, F., Kato, T., Kawamiya, M., Knorr, W., Lindsay, K., Matthews, H. D., Raddatz, T., Rayner, P., Reick, C., Roeckner, E., Schnitzler, K.-G., Schnur, R., Strassmann, K., Weaver, A. J., Yoshikawa, C., and Zeng, N.: Climate-carbon cycle feedback analysis: Results from the C^4MIP model intercomparison, J. Climate, 19, 3337–3353, 2006. 135, 139

Furevik, T., Bentsen, M., Drange, H., Kindem, I. K. T., Kvamstø, N. G., and Sorteberg, A.: Description and evaluation of the Bergen climate model: ARPEGE coupled with MICOM, Clim. Dynam., 21, 27–51, doi:10.1007/s00382-003-0317-5, 2003. 137

Gregory, J. M.: Long-term effect of volcanic forcing on ocean heat content. Geophys. Res. Lett., 37, L22701, doi:10.1029/2010GL045507, 2010. 135, 146

Hansen, J., Sato, M., Ruedy, R., Lacis, A., Asamoah, K., Borenstein, S., Brown, E., Cairns, B., Caliri, G., Campbell, M., Curran, B., de Castro, S., Druyan, L., Fox, M., Johnson, C., Lerner, J., McCormick, M. P., Miller, R. L., Minnis, P., Morrison, A., Pandolfo, L., Ramberran,

ESDD
2, 133–159, 2011

I., Zaucker, F., Robinson, M., Russell, P., Shah, K., Stone, P., Tegen, I., Thomason, L., Wilder, J., and Wilson, H.: A Pinatubo climate modeling investigation, in: The Mount Pinatubo eruption: Effects on the atmosphere and climate, edited by: Fiocco, G., Fua, D., and Visconti, G., NATO ASI Series, Ser I, 42, 219–231, 1996. 135

Houghton, R. A. and Hackler, J. L.: Carbon flux to the atmosphere from land-use changes, Trends: A compendium of data on global change, Carbon Dioxide Information Analysis Center, US Department of Energy, Oak Ridge, TN, USA, 2002. 139

Jones, C. D. and Cox, P. M.: Modeling the volcanic signal in the atmospheric CO_2 record, Global Biogeochem. Cy., 15, 453–465, 2001. 136, 142, 145

Lucht, W., Prentice, I. C., Myneni, R. B., Sitch, S., Friedlingstein, P., Cramer, W., Bousquet, P., Buermann, W., and Smith, B.: Climate control of the high-latitude vegetation greening trend and Pinatubo effect, Science, 296, 1687–1689, 2002. 145, 146

Maier-Reimer, E. and Hasselmann, K.: Transport and storage of CO_2 in the ocean-an inorganic ocean-circulation carbon cycle model, Clim. Dynam., 2, 63–90, 1987. 144

Maier-Reimer, E., Kriest, I., Segschneider, J., and Wetzel, P.: The HAMburg Ocean Carbon Cycle Model HAMOCC5.1 – Technical Description Release 1.1, Berichte zur Erdsystemforschung 14, ISSN 1614-1199, Max Planck Institute for Meteorology, Hamburg, Germany, 50 pp., 2005. 138

Marland, G., Boden, T. A., and Andres, R. J.: Global, regional, and national CO_2 emissions, Trends: A compendium of data on global change, Carbon Dioxide Information Analysis Center, US Department of Energy, Oak Ridge, TN, USA, 2005. 139

Matthews, H. D. and Caldeira, K.: Transient climate-carbon simulations of planetary geoengineering, P. Natl Acad. Sci. USA, 104, 9949–9954, doi:10.1073/pnas.0700419104, 2007. 146

Moore, J. C., Jevrejeva, S., and Grinsted, A.: Efficacy of geoengineering to limit 21st century sea-level rise, P. Natl. Acad. Sci. USA, 107(36), 15699–15703, doi:10.1073/pnas.1008153107, 2010. 136

Otterå, O. H.: Simulating the effects of the 1991 Mount Pinatubo volcanic eruption using the ARPEGE atmosphere general circulation model, Adv. Atmos. Sci., 25, 213–226, 2008. 138

Otterå, O. H., Bentsen, M., Bethke, I., and Kvamstø, N. G.: Simulated pre-industrial climate in Bergen Climate Model (version 2): model description and large-scale circulation features, Geosci. Model Dev., 2, 197–212, doi:10.5194/gmd-2-197-2009, 2009. 138

ESDD
2, 133–159, 2011

Otterå, O. H., Bentsen, M., Drange, H., and Suo, L.: External forcing as a metronome for Atlantic multidecadal variability, Nat. Geosci., 3, 688–694, doi:10.1038/ngeo955, 2010. 135, 136, 139

Rasch, P. J., Tilmes, S., Turco, R. P., Robock, A., Oman, L., Chen, C. C., Stenchikov, G. L., and Garcia, R. R.: An overview of geoengineering of climate using stratospheric sulphate aerosols, Philos. T. Roy. Soc. A, 366, 4007–4037, 2008. 136

Robock, A.: Volcanic eruptions and climate, Rev. Geophys., 38, 191–219, 2000. 136, 140

Robock, A., Oman, L., and Stenchikov, G. L.: Regional climate responses to geoengineering with tropical and Arctic SO_2 injections, J. Geophys. Res., 113, D16101, doi:10.1029/2008JD010050, 2008. 136

Robock, A., Bunzl, M., Kravitz, B., and Stenchikov, G. L.: A test for geoengineering?, Science, 327, 530–531,, 2010. 136

Sabine, C. L., Feely, R. A., Gruber, N., Key, R. M., Lee, K., Bullister, J. L., Wanninkhof, R., Wong, C. S., Wallace, D. W. R., Tilbrook, B., Millero, F. J., Peng, T.-H., Kozyr, A., Ono, T., and Rios, A. F.: The oceanic sink for anthropogenic CO_2, Science, 305, 367–371, 2004. 144

Sarmiento, J. L.: Atmospheric CO_2 stalled, Nature, 365, 697–698, 1993. 136, 146

Sitch, S., Smith, B., Prentice, I. C., Arneth, A., Bondeau, A., Cramer, W., Kaplan, J. O., Levis, S., Lucht, W., Sykes, M. T., Thonicke, K., and Venevsky, S.: Evaluation of ecosystem dynamics, plant geography and terrestrial carbon cycling in the LPJ dynamic global vegetation model, Global Change Biol., 9, 161–185, 2003. 138

Steinacher, M., Joos, F., Frölicher, T. L., Bopp, L., Cadule, P., Cocco, V., Doney, S. C., Gehlen, M., Lindsay, K., Moore, J. K., Schneider, B., and Segschneider, J.: Projected 21st century decrease in marine productivity: a multi-model analysis, Biogeosciences, 7, 979–1005, doi:10.5194/bg-7-979-2010, 2010. 144

Stenchikov, G., Delworth, T. L., Ramaswamy, V., Stouffer, R. J., Wittenberg, A., and Zeng, F.: Volcanic signals in oceans, J. Geophys. Res., 114, D16104, doi:10.1029/2008JD011673, 2009. 135, 136

Tjiputra, J. F., Assmann, K., Bentsen, M., Bethke, I., Otterå, O. H., Sturm, C., and Heinze, C.: Bergen Earth system model (BCM-C): model description and regional climate-carbon cycle feedbacks assessment, Geosci. Model Dev., 3, 123–141, doi:10.5194/gmd-3-123-2010, 2010. 135, 138, 139

ESDD
2, 133–159, 2011

Trenberth, K. E. and Dai, T.: Effects of Mount Pinatubo volcanic eruption on the hydrological cycle as an analog of geoengineering, Geophys. Res. Lett., 34, L15702, doi:10.1029/2007GL030524, 2007. 137

Wanninkhof, R.: Relationship between wind speed and gas exchange over the ocean, J. Geophys. Res., 97, 7373–7382, 1992. 143

Wigley, T. M. L.: A combined mitigation/geoengineering approach to climate stabilization, Science, 314, 452–545, 2006. 136

Zeebe, R. E. and Wolf-Gladrow, D. E.: CO_2 in seawater: Equilibrium, Kinetics, Isotops, Elsevier Oceanography Series, Amsterdam, The Netherlands, 65, 346 pp., 2001. 144

ESDD

2, 133–159, 2011

Table 1. List of performed experiments.

Experiment	Period	CO_2 emissions	Volcanic event frequency
REF	1850–2099	Historical and IPCC-A2	none
GEO_TAM	2020–2099	IPCC-A2	25-years (from 2025)
GEO_PIN	2020–2099	IPCC-A2	5-years (from 2020)

ESDD
2, 133–159, 2011

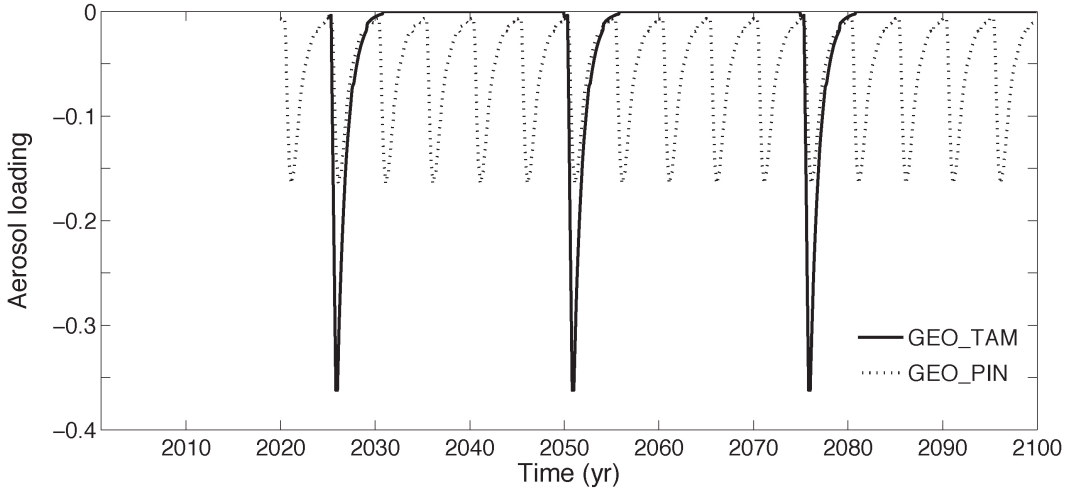

Fig. 1. Mean global aerosol loading (optical depth at 0.55 µm) applied to simulate the volcanic forcings in the GEO_TAM and GEO_PIN experiments.

ESDD
2, 133–159, 2011

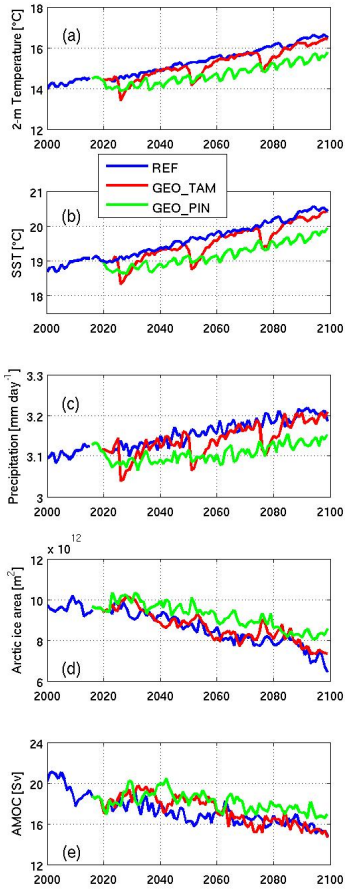

Fig. 2. Model projection of global mean **(a)** 2-m surface air temperature, **(b)** sea surface temperature, **(c)** precipitation, **(d)** summer (September) Arctic sea ice area, and **(e)** Atlantic Meridional Overturning Circulation (AMOC) strength for each experiments.

ESDD
2, 133–159, 2011

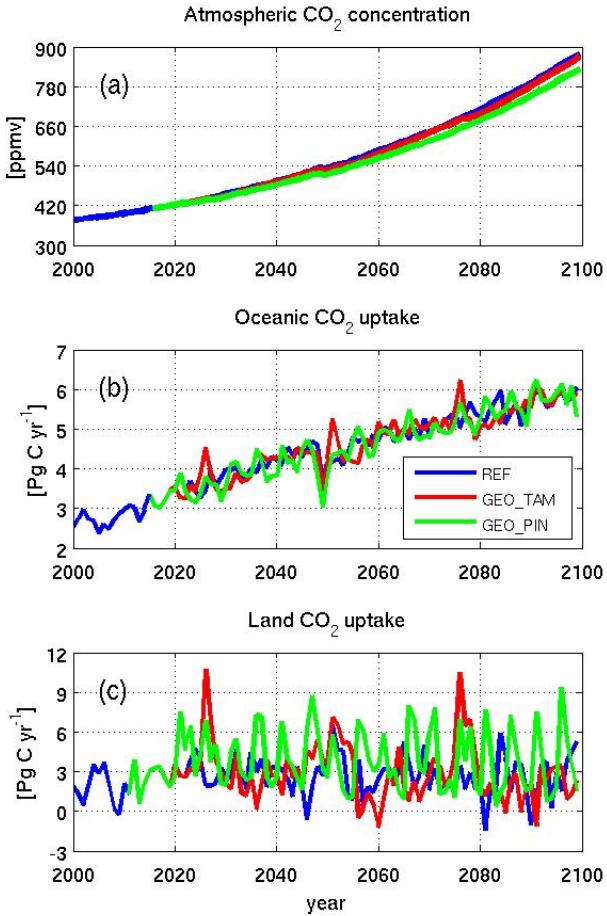

Fig. 3. Model projection of annual mean **(a)** atmospheric CO_2 concentration, **(b)** oceanic carbon uptake, and **(c)** terrestrial carbon uptake over the 2000–2099 period.

ESDD
2, 133–159, 2011

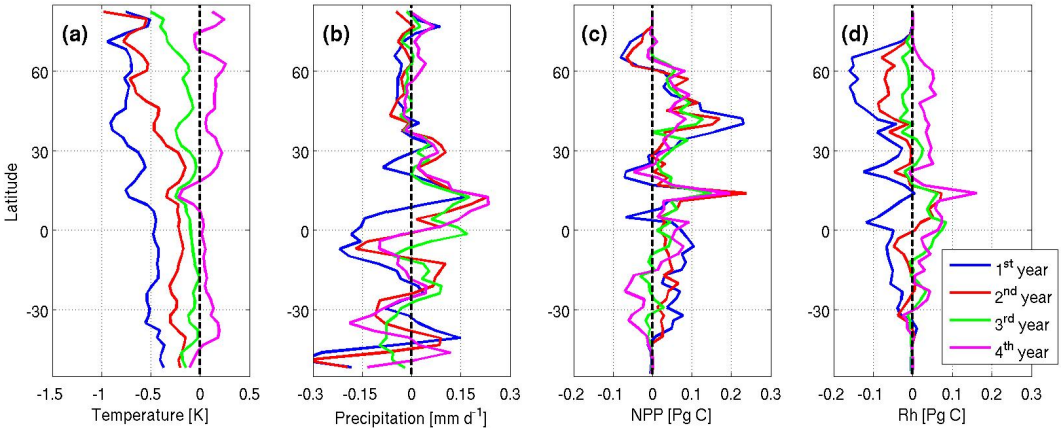

Fig. 4. Latitudinal change in annual mean **(a)** temperature, **(b)** precipitation, **(c)** net primary production, and **(d)** heterotrophic respiration over land following the volcanic eruption forcing in GEO_PIN. Colors represent different years immediately follow the eruptions.

ESDD
2, 133–159, 2011

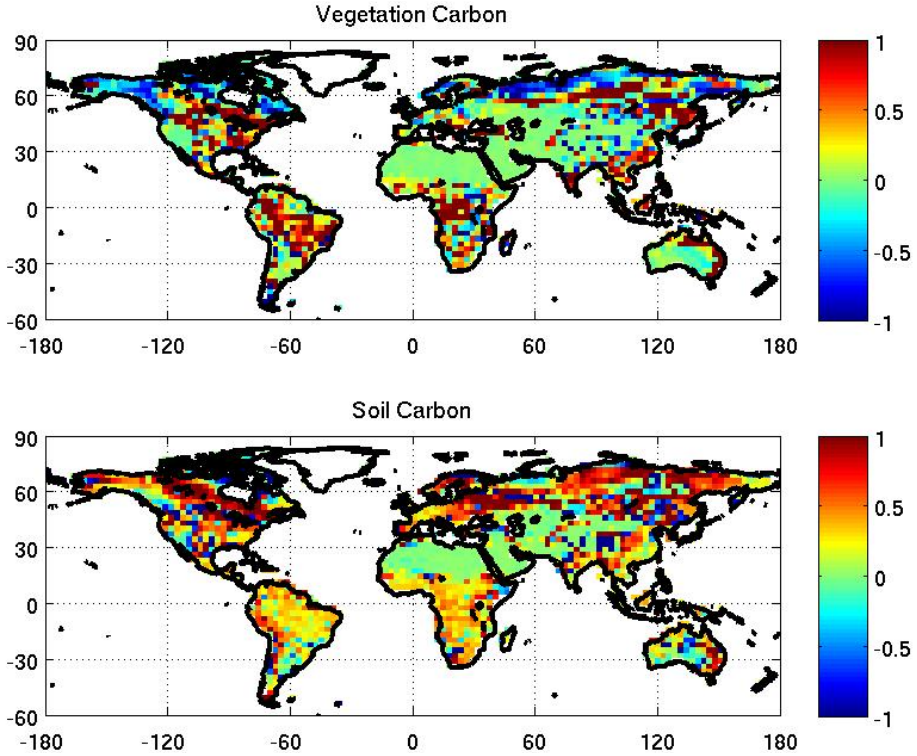

Fig. 5. Mean changes (GEO_PIN minus REF) in total land (top) vegetation and (bottom) soil carbon content due to additional volcanic forcings computed over 2090–2099 period. Units are in [Kg C m^{-2}].

ESDD
2, 133–159, 2011

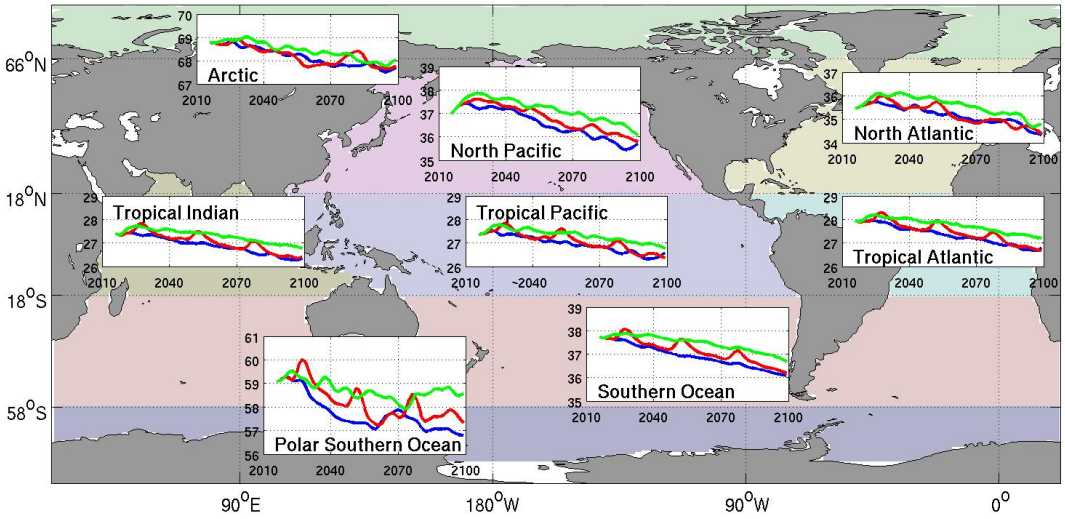

Fig. 6. Regional evolution of solubility of CO_2 gas in seawater from 2020 to 2099 period. Plotted here are the five-year running means from (blue-lines) REF, (red-lines) GEO_TAM, and (green-lines) GEO_PIN experiments. Units are in [mmol l^{-1} ppm^{-1}].Regions are defined as follow: Arctic (ARC, >66° N), North Atlantic (NAT, 18° N–66° N), North Pacific (NPA, 18° N–66° N), Tropical Atlantic (TAT, 18° S–18° N), Tropical Pacific (TPA, 18° S–18° N), Tropical Indian (TIN, 18° S–25° N), subtropical Southern Ocean (SOC1, 58° S–18° S), high latitude Southern Ocean (SOC2, >58° S).

ESDD
2, 133–159, 2011

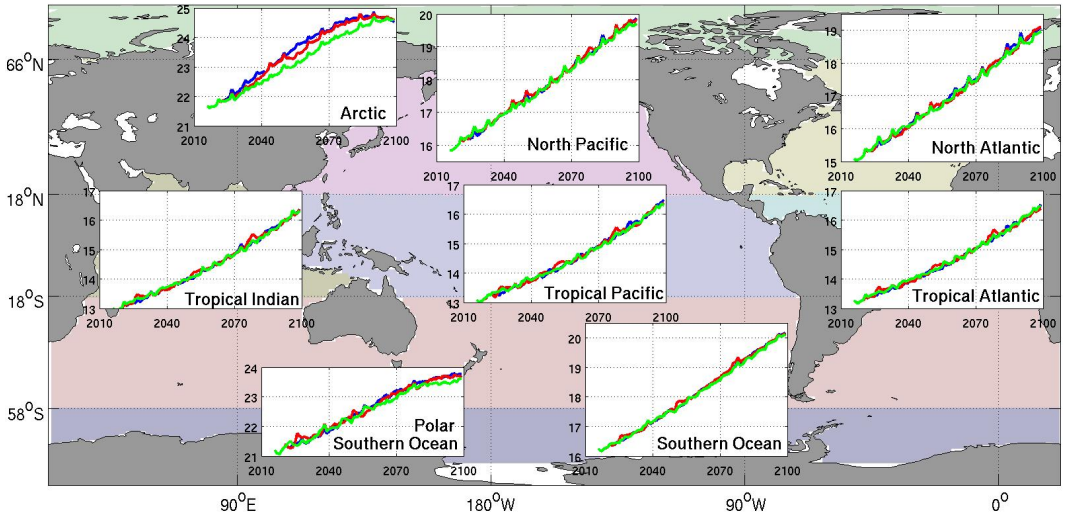

Fig. 7. Similar to Fig. 6 for Revelle factor.

ESDD
2, 133–159, 2011